

Mass conservation issues of moving interface flows modelled by the interface capturing approach

A. Kačeniauskas

Vilnius Gediminas Technical University, Saulėtekio 11, 10223 Vilnius, Lithuania, E-mail: arnka@fm.vtu.lt

1. Introduction

Many industrial applications of mechanical engineering involve moving interface flows. Numerous examples include actual problems such as coating process, metal forming, sluice gates, tank sloshing and dam break. Numerical simulation of moving interface flows is extremely complex, since it involves the solution of the incompressible Navier-Stokes equations coupled with moving interface tracking. The numerical approach has to identify the unknown interface, to follow its kinematics and to resolve a strong coupling between the interface propagation and dynamics of the continuum.

Over the past 30 years, researchers have put a lot of effort into developing various numerical methods to simulate the moving interface flows governed by the Navier-Stokes equations. All numerical methods for modelling of the moving interface flows are based on interface tracking approach or interface capturing approach. In former, the liquid region is subdivided by a mesh, while each cell is deformed according to the movement of the interface and computed velocities. The earliest works [1] were based on the Lagrangian description of motion. However, this approach requires remeshing procedures to avoid of computation failure due to serious distortion of cells or elements [2]. Various interface tracking methods [3, 4] for attaching the interface to a mesh surface were developed during the past decades using the finite element method (FEM). These methods are unable to cope naturally with interface interacting with itself by folding or rupturing.

In the interface capturing approach, the mesh remains fixed and moving interface can not be directly defined by the mesh nodes. Therefore, additional technique is necessary to define the areas occupied by fluid or gas on either side of the interface. The marker-and-cell method [5], the volume of fluid method [6] and the level set method [7] are well known methods using the interface capturing approach. These methods require no geometry manipulations after the mesh is generated and can be applied to interfaces of a complex topology [8]. However, the location of the interface is not explicit and, sometimes, the appropriate boundary conditions cannot be prescribed with a required accuracy.

The volume of fluid methods are very efficient and practical [9], therefore, they are implemented in a lot of commercial codes using the finite volume method. The level set method is based on finite difference schemes. The mathematical model of the level set method is very universal, but the numerical implementation of reinitialization procedures [10] is quite complicated and requires large computational resources [11]. A pseudo-concentration method [12] often used with the FEM is an interesting alternative for the level set method. This method uses a

pseudo-concentration function defined in the entire domain and solves a hyperbolic equation to determine the moving interface [13]. In the most cases, the pseudo-concentration method is more efficient than the level set method, because it uses simpler front reconstruction techniques. The FEM has become a powerful tool for solving many scientific and engineering applications, therefore, the demand for further investigation of the ICT and implementation in commercial FEM codes is rapidly growing [14].

The main concern with the interface capturing approach has been sustaining global mass conservation in long-time integrations [15]. It was observed that numerical diffusion introduces a normal motion proportional to the local curvature of the interface, which leads to non-physical mass transfer between the two fluids. The interface sharpening techniques [16] employed together with the pseudo-concentration method include various numerical parameters, which values might depend on the mesh size, the time step and the physics of the flow. Thus, the choice of the numerical schema, the mass correction procedure and numerical parameters remains state of the art problem.

2. Equations governing the flow

The laminar and Newtonian flow of viscous and incompressible fluids is considered. It is governed by the Navier-Stokes equations (the Eulerian reference frame)

$$\rho \left(\frac{\partial u_i}{\partial t} + u_j \frac{\partial u_i}{\partial x_j} \right) = \rho F_i + \frac{\partial \sigma_{ij}}{\partial x_j} \quad (1)$$

$$\frac{\partial u_i}{\partial x_i} = 0 \quad (2)$$

where u_i are the velocity components; ρ is the density; F_i are the gravity force components and σ_{ij} is stress tensor

$$\sigma_{ij} = -p\delta_{ij} + \mu \left(\frac{\partial u_i}{\partial x_j} + \frac{\partial u_j}{\partial x_i} \right) \quad (3)$$

where μ is dynamic viscosity coefficient; p is pressure and δ_{ij} is Kronecker delta.

Slip boundary conditions for velocity are prescribed on rigid walls

$$u_i n_i = 0 \quad (4)$$

where n_i are components of a unit normal vector. This is usual choice of boundary conditions used for modelling of moving interface flows. However, the boundary conditions (4) are not able accurately to capture behaviour of the flow

near walls or handle air bubbles near the corners.

The stress dependent boundary conditions [17], used in mould filling problems, are prescribed on permeable walls

$$\text{if } n_i \sigma_{ij} n_j > 0 \text{ then } \sigma_{ij} n_j = 0 \quad (5)$$

$$\text{if } n_i \sigma_{ij} n_j < 0 \text{ then } u_i n_i = 0 \text{ and } n_i \sigma_{ij} t_j = 0 \quad (6)$$

where t_j are components of a unit tangent vector. The boundary conditions (5), (6) can resolve problems of incompressible flows related with air bubbles or flow suddenly separating from the wall. The detailed discussion on stress dependent boundary conditions and their implementation can be found in the work [18].

The propagation of moving interface is described by the pseudo-concentration method based on the interface capturing approach. The evolution of the interface is governed by the time dependent convection equation

$$\frac{\partial \varphi}{\partial t} + u_j \frac{\partial \varphi}{\partial x_j} = 0 \quad (7)$$

where φ is pseudo-concentration function serving as a marker identifying fluids A and B with densities ρ_A and ρ_B and viscosities μ_A and μ_B . Thus, in the Navier-Stokes Eqs. (1)-(3), the density and viscosity are defined as

$$\rho = \varphi \rho_A + (1 - \varphi) \rho_B \quad (8)$$

$$\mu = \varphi \mu_A + (1 - \varphi) \mu_B \quad (9)$$

while $\varphi=1$ for fluid A and $\varphi=0$ for fluid B. The initial conditions defined on the entire solution domain should be prescribed for the Eq. (7).

The space-time Galerkin least squares finite element method [3] is applied as a general-purpose computational approach to solve the partial differential Eqs. (1)-(3), (7). Equal order bilinear shape functions are used for both the pressure and velocity components as well as for the pseudo-concentration function. The detailed description of variational formulation and stabilisation parameters can be found in the work [19].

3. Mass correction technique

The bottleneck of the interface capturing approach is numerical diffusion, which smears the sharpness of the moving front and causes problems with mass conservation. The function defining the interface undergoes some diffusion as it is advected through the computational domain. The pseudo-concentration function should be reconstructed in order to preserve mass conservation. In this paper, the investigated mass correction or interface sharpening technique is presented in the work [20]. The values of the pseudo-concentration function φ are replaced by the values of the reconstructed function ϕ , considering the following formula:

$$\phi = c^{1-a} \varphi^a, \quad 0 \leq \varphi \leq c \quad (10)$$

$$\phi = 1 - (1 - c)^{1-a} (1 - \varphi)^a, \quad c < \varphi \leq 1 \quad (11)$$

where the parameter c represents mass conservation level, while a governs sharpness of the moving interface. The

detailed discussion on interface sharpening parameters has been presented in the work [20]. In this work, the value of the coefficient a is considered to be equal 1.4.

The formulas (10), (11) can be applied only if $0 \leq \varphi \leq 1$. In practical application of the Galerkin Least Squares stabilizing method to the complex problems governed by convective transport, some overshoots and undershoots are observed [21]. In order to apply the developed interface reconstruction procedure, a simpler limiter should be implemented

$$\phi = \min[\max[\varphi, 0], 1] \quad (12)$$

It removes the overshoots and prevents the field from undesirable numerical oscillations.

In this paper, we will focus our attention on mass conservation issues. Insignificant numerical errors, which result in slight nonphysical mass transfer between the two fluids, may lead to significant errors in long-term time integration of the problem. In order to overcome this difficulty and to preserve mass conservation, the values of coefficient c should be computed considering precise mass distribution in the interface region. At any time, mass conservation for fluid A in the solution domain Ω can be described by the formula

$$M_A = \rho_A \int_{\Omega} \phi d\Omega \quad (13)$$

where M_A is the initial mass of the fluid A. The equation for determining c can be obtained by substituting ϕ from formulas (10), (11) to Eq. (13). Assuming that a is given and constant, the resulting equation for mass conservation can be written as follows:

$$K_1 c^{1-a} - K_2 (1-c)^{1-a} = M_A - M_A^\varphi \quad (14)$$

where coefficient K_1 is defined on the narrow band of the moving interface $0 \leq \varphi \leq c$

$$K_1 = \rho_A \int_{\Omega} \varphi^a d\Omega \quad (15)$$

Coefficient K_2 is computed on the remaining part of the interface $c < \varphi \leq 1$

$$K_2 = \rho_A \int_{\Omega} (1 - \varphi)^a d\Omega \quad (16)$$

Coefficient M_A^φ represents the current mass of the fluid A, defined by the values of the φ function $c < \varphi \leq 1$

$$M_A^\varphi = \rho_A \int_{\Omega} \varphi d\Omega \quad (17)$$

The right side of Eq. (14) means mass deviation from the initial mass M_A . Despite the fact that only one fluid is explicitly presented in Eqs. (14)-(17), the described procedure conserves mass for each fluid. In the solved problems, the fluid A is heavy (water), while the fluid B is relatively light (air). Mass correction applied to the heavier fluid A helps to ensure maximal accuracy of the procedure.

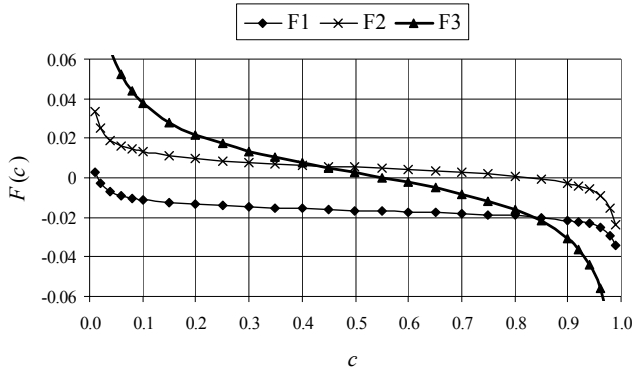


Fig. 1 Character of nonlinear function $F(c)$

The final values of mass conservation level c are obtained solving one-dimensional nonlinear Eq. (14). The nonlinear function $F(c)$ can be written as follows

$$F(c) = K_1 c^{1-a} - K_2 (1-c)^{1-a} - M_A + M_A^\varphi \quad (18)$$

Fig. 1 illustrates the character of several $F(c)$ curves. The investigated character of $F(c)$ is predefined by formulas (10), (11). $F1$ is obtained when mass loss is observed and $M_A - M_A^\varphi > 0$. The positive value of the right hand side of Eq. (14) indicates that the nonlinear solution is between 0.0 and 0.5. Formulas (10), (11) also define that it is necessary to decrease c value below 0.5 in order to increase mass. On the opposite, such curves like $F2$ are obtained when computed mass is increased above initial fluid mass M_A and $M_A - M_A^\varphi < 0$. In this case, the solution of nonlinear Eq. (14) is between 0.5 and 1.0.

The secant method has been chosen for efficient solution of nonlinear Eq. (14), because it is very suitable for predefined character of nonlinear curves $F(c)$. This method requires two initial values. The first initial value c_1 has been considered to be equal 0.5, which indicates satisfactory mass conservation. The second initial value c_2 is computed considering the sign of the right hand side of Eq. (14). c_2 is increased (decreased) by an arbitrary value dc if $M_A - M_A^\varphi < 0$ (> 0). If the root is between c_1 and c_2 , then $F(c_1) \cdot F(c_2) < 0$. If not, then c_2 value should be further increased (decreased). Initial values c_1 and c_2 should be chosen to lie as close to the solution as possible, therefore, dc value can be changed during the process as well as c_1 value. In the most cases, the solution is very close to 0.5, therefore, dc is initialized to 0.1. In extreme cases, when the topology of moving interface changes very rapidly or sharpening is performed very seldom, the root can be close to the end point of considered interval. Then dc is reduced to 0.01 (or even smaller value) and suitable value for c_2 is obtained. In such cases, the approximate c values like 0.1 or 0.9 can be successively applied for interface sharpening in order to avoid solving nonlinear equation and to reduce computing time.

In the investigated cases, the convergence of the secant method is super-linear, because the root is simple and $F(c)$ is twice continuously differentiable. The nonlinear algorithm usually converges after two or three iterations. The extreme cases (curve $F3$) will be discussed in the following section. Other general iterative methods like Newton-Raphson can also be applied to the solution of Eq.

(14), but they should be enough flexible to deal with complicated nonlinear solutions or special algorithm should be designed for exploiting the predefined character of the curve $F(c)$.

4. Description of dam break problem

The developed mass correction technique has been applied for modelling a dam break flow in a confined domain. The dam break problem including the breaking wave phenomena has been the subject of extensive research for a long time [6, 22, 23]. However, the universal, accurate and efficient numerical technique for breaking wave simulation attracts big attention of research community and software developers. Measurements of the exact interface shape are not available, but some secondary data such as reduction of the water column height can be employed for quantitative comparison of the obtained results [22]. The validation of the obtained numerical solution by quantitative comparison with experimental measurements can be found in the works [20, 21].

The geometry of the solution domain is shown in Fig. 2. A rectangular cavity with dimensions $0.09 \text{ m} \times 0.03 \text{ m}$ is considered ($a=0.015 \text{ m}$). At initial time $t=0.0 \text{ s}$, water is confined in the left half of the cavity. Later it is the subject of vertical gravity ($g=9.81 \text{ m/s}^2$) and free to move. Water density is $\rho_A=1000 \text{ kg/m}^3$, the dynamic viscosity coefficient is $\mu_A=0.01 \text{ kg/(m s)}$. The density of air is taken to be $\rho_B=1 \text{ kg/m}^3$ and the dynamic viscosity coefficient is $\mu_B=0.0001 \text{ kg/(m s)}$. The slip boundary conditions Eq. (4) have been applied to the bottom and sides of the reservoir. The stress dependent boundary conditions (5)-(6) have been prescribed on the upper wall. Two structural finite element meshes of different resolution (120×40 and 240×80) are employed for computations. The investigated time interval $t=[0.0; 0.3] \text{ s}$ is divided to 300 and 600 time steps, respectively.

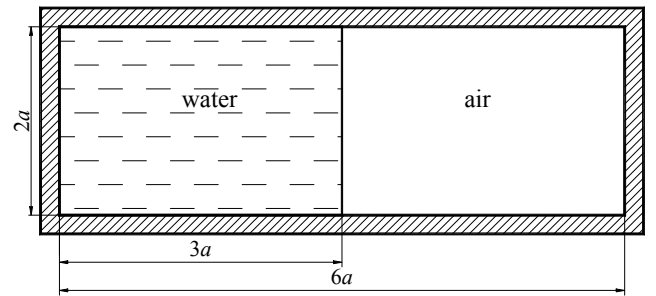


Fig. 2 Geometry of dam break problem

5. Numerical results and discussions

The discussed mass correction technique has been implemented in the FEM code FEMTOOL [19, 24] designed for coupled problems of Computational Fluid Dynamics. Numerical experiments have been performed on the LitGRID clusters (<http://www.litgrid.lt/>).

Mass conservation is one of the most important tasks for any numerical scheme. In order to evaluate global mass conservation, exact mass values should be computed

$$M_{TOT}^\varphi = \sum_{e=1}^{ne} \sum_{p=1}^{np} G_p^e \rho_p^\varphi \quad (19)$$

where M_{TOT}^o is total current mass; G_p^e are Gauss coefficients of the e -th finite element; ρ_p^o denotes the non-smoothed density value at p -th Gauss point computed considering nodal values of the pseudo-concentration function φ ; ne is total number of finite elements; np is total number of Gauss points. The global mass error Me is computed considering the following formula

$$Me = M_{TOT}^o - M_{INI} \quad (20)$$

where M_{INI} is total initial mass. Negative Me values indicates mass loss, while positive Me values reflects undesirable mass increase.

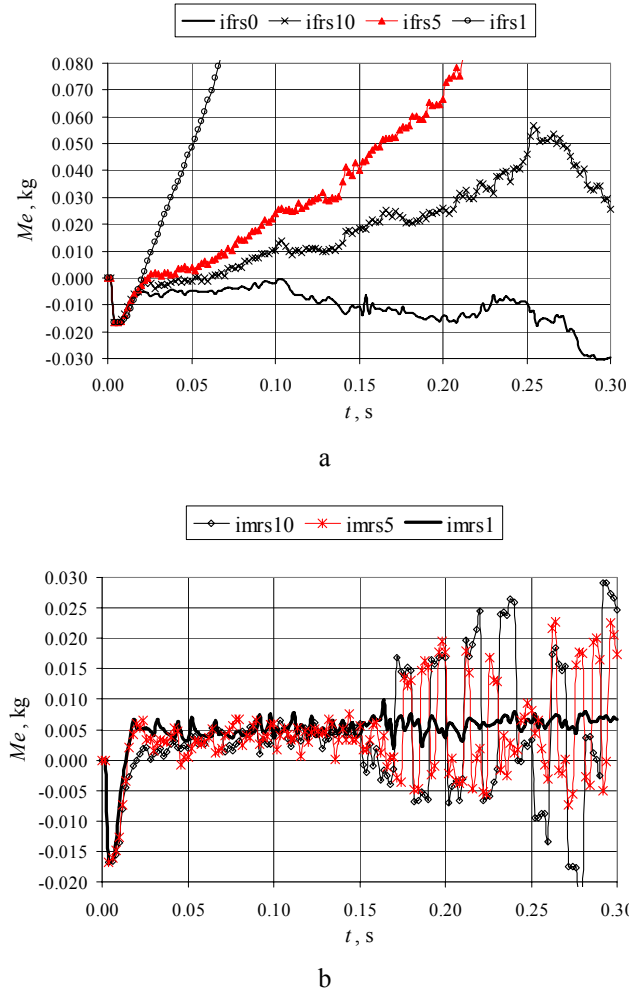


Fig. 3 Time evolution of global mass for different strategies of interface sharpening: a - without mass correction; b - with mass correction

Most of the computations were performed on coarser finite element mesh (120x80), because it is more challenging task for the mass correction. Fig. 3 presents time evolution of the global mass error. The curves plotted in Fig. 3, illustrate mass conservation obtained without mass correction technique. The curve ifrs0 is obtained without any interface sharpening. The mass loss is equal to 2.42% of the initial mass $M_{INI} = 1.34$ kg. The curves ifrs10, ifrs5 and ifrs1 are computed performing regular sharpening of the front (ifrs) at each 10, 5 and 1 time steps, respectively. Fig. 3, a shows that the interface sharpening

changes the character of time evolution of the global mass conservation. However, it is obvious that the interface sharpening without mass correction is not able to preserve mass conservation. The global mass error is equal 4.24% (the curve ifrs10) or 8.35% (the curve ifrs5). It can exceed even 43% in extremely unsuccessful case of the curve ifrs1.

Fig. 3, b illustrates the initial application of the mass correction technique at regular sharpening of the front (imrs). The allowable mass error is considered to be equal 0.005 kg, which is quite strict requirement equal less than 0.5% of initial mass. The curves imrs10, imrs5 and imrs1 are obtained by using different interface sharpening frequencies 10, 5 and 1, respectively. Only mass correction at each time step (the curve imrs1) preserves the defined level of mass conservation. However, frequent interface sharpening distorts the interface smoothness and can produce “staircases”, when the interface adapts to the finite elements mesh [20]. Lower sharpening frequencies produce large oscillations of the global mass error. It is obvious that oscillations starting at time $t=0.15$ s need further detailed investigation.

Fig. 4 illustrates physical behaviour of the flow in complex cases that are heavily handled by the mass correction technique. The pseudo-concentration function value 0.5 represents exact shape of the moving interface. Grey colours show the transition region between different fluids. Fig. 4, a shows flow separation from the upper wall by one row of finite elements, when $t=0.003$ s. Complex numerical handling of this phenomenon by stress dependent boundary conditions (5)-(6) causes sudden mass loss in the third time step (Fig. 3), which is successfully repaired by mass correction during 7-10 subsequent time steps. Figs. 4, b and 4, c illustrate flow separation from the upper wall, when $t=0.150$ s. Capturing of the long and narrow “tongue” is a complicated process (Fig. 3) on the coarse finite element mesh.

Further examination of the undesirable oscillations showed that they are caused by nonconvergent nonlinear algorithm and unpredictable behaviour of the mass correction technique in such extreme cases. Fig. 5 shows time evolution of variable nc , which counts possible non-convergent cases of the mass correction technique. Special cases, when sharpening is not performed, but non-convergent situation is detected, are also evaluated in this variable. nc values of the curves imrs10 and imrs5 are unallowably high.

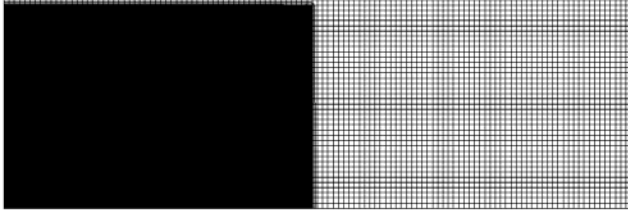
It was discovered that the nonlinear function $F(c)$ changes its predefined character in such extreme cases (Fig. 1). The nonlinear solution of the curve F3 lies between 0.5 and 1.0 in spite of the positive value of the right hand side of Eq. (14), which indicates that the non-linear solution should be between 0.0 and 0.5. In such unexpected cases, the second initial value c_2 is chosen to be in the wrong interval, therefore, nonlinear algorithm does not converge. It is very easy to observe that nonlinear solution is very close to the initial value $c_1=0.5$, but it is on the opposite side. The nonlinear algorithm can be easily modified, but first of all an indicator, identifying such unexpected numerical phenomena, should be discovered.

Detailed investigation showed that the averaged mass error Me_{AVE} can be very useful for this purpose. It is computed by the following formula

$$Me_{AVE} = M_{AVE}^{\phi} - M_{INT} \quad (21)$$

where M_{AVE}^{ϕ} is averaged current mass computed considering density values averaged by the formula (8). M_{AVE}^{ϕ} is computed by the following formula

$$M_{AVE}^{\phi} = \sum_{e=1}^{ne} \sum_{p=1}^{ng} G_p^e (\phi_p^e \rho_A + (1 - \phi_p^e) \rho_B) \quad (22)$$



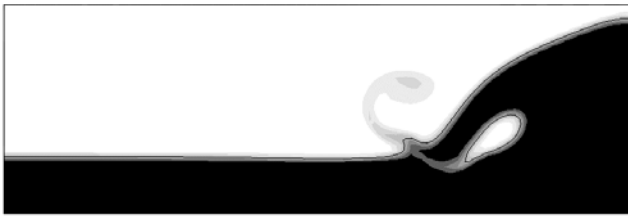
a



b



c



d



e

Fig. 4 Dam break flow visualization by the pseudo-concentration function on the stationary finite element mesh: a - $t=0.003$ s; b - $t=0.150$ s; c - $t=0.175$ s; d - $t=0.267$ s; e - $t=0.275$ s

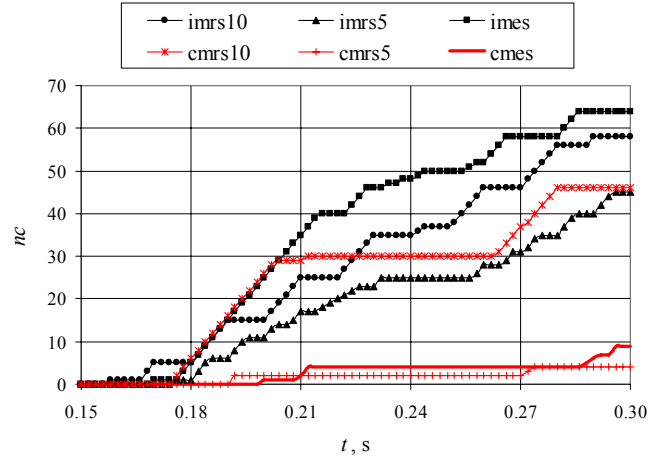


Fig. 5 Time evolution of the nonconvergence number nc of mass correction technique

where ϕ_p^e is ϕ value at p -th Gauss point of e -th finite element. Large density ratios might cause numerical oscillations at the interface [21], therefore, in a finite element constant density is employed for computation of the local finite element matrices. It was discovered that the averaged mass error Me_{AVE} has the opposite sign than the global mass error Me in the cases, when nonlinear algorithm of mass correction technique does not converge. It can be explained by spreading grey-colored zone, which indicates the growth of the area occupied by the moving interface. Stable numerical handling of increasing interface thickness is challenging task for any interface capturing technique.

The algorithm for nonlinear solution of mass conservation Eq. (14) was corrected considering the special case indicator based on the sign of expression $Me * Me_{AVE}$. Instead of looking for nonlinear solution on the opposite side of the middle value $c_1=0.5$, sharpening with predefined value $c=0.5$ is performed. Thus, the interface thickness is reduced. The resulting situation becomes more convenient for handling in subsequent time steps. Fig. 5 illustrates significant improvement in convergence. The curves cmrs10 and cmrs5 are obtained by using corrected algorithm of mass conservation and the regular interface sharpening frequencies 10 and 5, respectively. Nonlinear algorithm always converges, when the interface sharpening is performed in each time step (imrs1 and cmrs1), because the interface thickness becomes very small.

Fig. 6 illustrates time evolution of the global mass error for different cases of mass correction handling. Large oscillations of the global mass error are not observed in the curves cmrs10 and cmrs5. Seldom mass correction is not able to preserve the defined level of mass conservation (the curve cmrs10 in Fig. 6, a). The curves imes and cmes are obtained governing the interface sharpening only by the global mass error without interface sharpening at regular time intervals. It is worth to note that drastic improvement of nonlinear convergence is observed comparing the curves imes and cmes (corrected nonlinear algorithm) in Fig. 5. The interface sharpening handled by the global mass error preserves mass even better than the interface sharpening and mass correction performed at regular time intervals (the curves cmes and cmrs5 in Fig. 6, b). The frequent mass correction is necessary at the beginning of the time interval, when $t=[0.003; 0.015]$ s, which was discussed above and illustrated in Fig. 4, a. When $t=[0.260; 0.275]$,

the backward moving wave folds over and a small amount of air is trapped (Figs. 4, d and 4, e). It is very difficult to handle the merging interface in such case, therefore, the frequent interface sharpening and mass correction is required. Computing cmes the mass correction together with the interface sharpening was performed 57 times. The regular interface sharpening enriched with the mass correction required 60 times in case of cmrs5. Both strategies required similar amount of computational resources and produced results of similar accuracy.

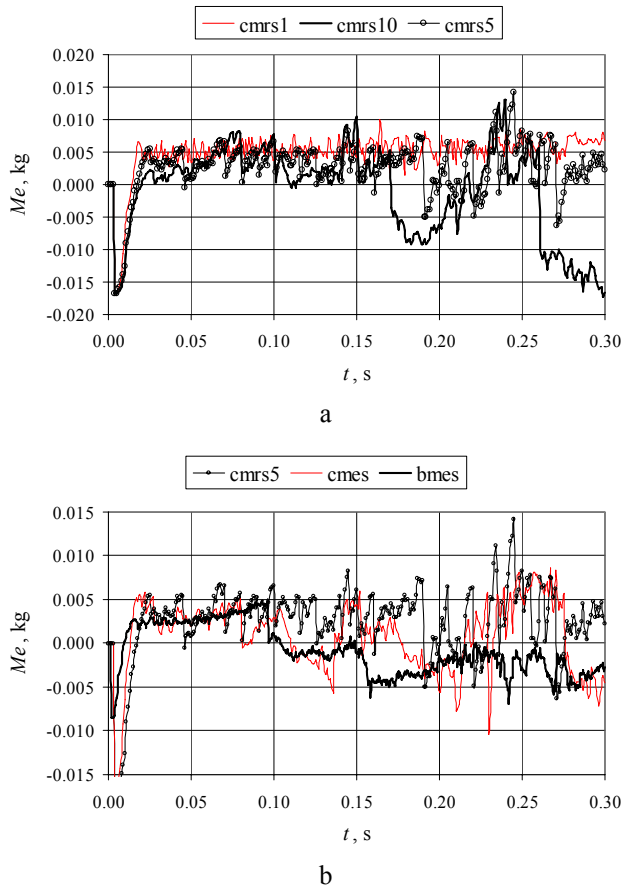


Fig. 6 The global mass conservation in time: a - the interface sharpening and mass correction performed at regular time intervals, b - the interface sharpening and mass correction handled by the mass error Me

Finally, mass conservation was investigated on the denser finite element mesh 240×80 by using 600 time steps. The interface sharpening was governed only by the global mass error (the curve bmes). The same allowable mass error was prescribed. As was expected, handling of mass conservation was easier in such convenient case. The mass conservation technique was applied only 22 times. At the beginning of the time interval the observed mass loss was smaller (Fig. 7, a). Moreover, it was very quickly eliminated by mass correction. However, the total computing time of larger problem (bmes) was 11.8 times longer than that of the smaller one (cmes).

6. Conclusions

In this paper, the development of the mass correction technique for viscous incompressible moving interfaces flows modelled by interface capturing approach has

been described. The regular interface sharpening without mass correction is not able to preserve mass conservation. The interface sharpening and the mass correction governed by different strategies require similar amount of computational resources and produce results of similar accuracy. Quick topological changes of the moving interface flow causes difficulties for the nonlinear solution of the mass conservation equation. The employed algorithm should exploit predefined character of the nonlinear solution and carefully take care of the extreme cases, when this character can be violated. The accurate numerical solution of the complex problem including breaking waves proves that the developed mass correction technique is capable of preserving mass conservation at the required level.

Acknowledgement

The computational resources provided by the LitGRID (Ministry of Education and Science, ISAK-1570) are gratefully acknowledged. Flow visualization tool is developed in GridTechno (Lithuanian State Science and Studies Foundation, B-07043) project and FP7 project BalticGrid-II.

References

1. **Hirt, C.W., Cook, J.L., Butler, T.D.** A Lagrangian method for calculating the dynamics of an incompressible fluid with free surface. -J. Computational Physics, 1970, No5(1), p.103-124.
2. **Radovitzky, R., Ortiz, M.** Lagrangian finite element analysis of newtonian fluid flows. -Int. J. Numerical Methods in Engineering, 1998, No43(4), p.607-619.
3. **Masud, A., Hughes, T.J.R.** A Space - time Galerkin/least - squares finite element formulation of the Navier-Stokes equations for moving domain problems. -Computational Methods in Applied Mechanics and Engineering, 1997, No146(1-2), p.91-126.
4. **Del Pin, F., Idelsohn, S., Oñate, E., Aubry, R.** The ALE/Lagrangian particle finite element method: a new approach to computation of free-surface flows and fluid-object interactions. -Computers & Fluids, 2007, No36(1), p.27-38.
5. **Harlow, F.H., Welch, J.E.** Numerical calculation of time - dependent viscous incompressible flow. -J. Physics of Fluids, 1965, No8(12), p.2182-2189.
6. **Hirt, C.W., Nichols, B.D.** Volume of fluid (VOF) method for the dynamics of free boundaries. -J. Computational Physics, 1981, No39(1), p.201-225.
7. **Osher, S., Sethian, J.A.** Fronts propagating with curvature - dependent speed: algorithms based on Hamilton-Jacobi formulation. -J. Computational Physics, 1988, No79(1), p.12-49.
8. **Löhner, R., Yang, C., Oñate, E.** On the simulation of flows with violent free surface motion. -Computer Methods in Applied Mechanics and Engineering, 2006, No195(41-43), p.5597-5620.
9. **Mencinger, J., Žun, I.** On the finite volume discretization of discontinuous body force field on collocated grid: application to VOF method. -J. Computational Physics, 2007, No221(2), p.524-538.
10. **Sussman, M., Fatemi, E.** An efficient, interface preserving level set re-distancing algorithm and its appli-

- cation to interfacial incompressible fluid flow. -SIAM J. Scientific Computations, 1999. No20(4), p.1165-1191.
11. **Kačeniauskas, A.** Two - phase flow modelling by the level set method and finite elements. -Energetika, 2000, No4, p.22-31.
 12. **Thompson, E.** Use of pseudo-concentration to follow creeping viscous flow during transient analysis. -Int. J. for Numerical Methods in Fluids, 1986, No 7(2), p.749-761.
 13. **Lewis, R.W., Ravindran, K.** Finite element simulation of metal casting. -Int. J. for Methods in Engineering, 2000, No47, p.29-59.
 14. **Tezduyar, T.E.** Finite elements in fluids: Special methods and enhanced solution techniques. -Computers & Fluids, 2007, No36(2), p.207-223.
 15. **Di Pietro, D.A., Lo Forte, S., Parolini, N.** Mass preserving finite element implementations of the level set method. -Applied Numerical Mathematics, 2006, No56(9), p.1179-1195.
 16. **Aliabadi, S., Tezduyar, T.E.** Stabilized - finite-element/interface - capturing technique for parallel computation of unsteady flows with interfaces. -Computational Methods in Applied Mechanics and Engineering, 2000, No 190(3-4), p.243-261.
 17. **Dieterlen, R., Maronnier, V., Picasso, M., Rappaz, J.** Numerical simulation of free surface computational mechanics. New Trends and Applications, Eds. S. Idelson, E. Onate, E. Dvorkin, Barcelona, 1998.-13p.
 18. **Kačeniauskas, A., Kutas, R.** Implementation of stress dependent boundary conditions in FEM code for coupled problems. Submitted to Informacinės technologijos ir valdymas, 2008.
 19. **Kačeniauskas, A., Rutschmann, P.** Parallel FEM software for CFD problems. -Informatica, 2004, No3(15), p.363-378.
 20. **Kačeniauskas, A.** Development of efficient interface sharpening Procedure for Viscous Incompressible Flows. Submitted to Informatica, 2008.
 21. **Kačeniauskas, A.** Dam break flow simulation by the pseudo-concentration method. -Mechanika. -Kaunas: Technologija, 2005, Nr.1(51), p.39-43.
 22. **Martin, J.C., Moyce, W.J.** An experimental study of the collapse of liquid columns on a rigid horizontal plane. -Philos. Trans. Roy. Soc. London, 1952, NoA244, p.312-324.
 23. **Quecedo, M., Pastor, M., Herreros, M.I., Merodo, J.A.F., Zhang, Q.** Comparison of two mathematical models for solving the dam break problem using the FEM method. -Computer Methods in Applied Mechanics and Engineering, 2005, No194(36-38), p.3984-4005.
 24. **Kačianauskas, R., Rutschmann, P.** Implementation and testing of finite elements for Navier-Stokes equations in the FEMTOOL code. -Mechanika, -Kaunas: Technologija, 1996, Nr.2(5), p.5-11.

A. Kačeniauskas

DVIPUSIŲ PAVIRŠIŲ TĖKMĖS, MODELIOJAMOS REMIANTIS NEIŠREIKŠTINIO PAVIRŠIAUS KONCEPCIJA, MASĖS TVERMĖS PROBLEMOS

Re z i u m ė

Straipsnyje pateikiama masės tvermės palaikymo technologija, skirta klampioms nespūdžioms dvipusių paviršių tėkmėms modeliuoti. Sugriuvusios užtvankos uždavinys sprendžiamas pseudokoncentracijos metodu, pagrįstu neišreikštinio paviršiaus koncepcija. Pateikiami detalūs skaitiniai netiesinės masės tvermės lygties sprendimo tyrimai. Nagrinėjamos įvairios paviršiaus rekonstrukcijos valdymo strategijos. Masės tvermės palaikymo technologija testuota dviem skirtingos rezoliucijos baigtinių elementų tinklais.

A. Kačeniauskas

MASS CONSERVATION ISSUES OF MOVING INTERFACE FLOWS MODELLED BY THE INTERFACE CAPTURING APPROACH

S u m m a r y

The paper describes the development of the mass correction technique for viscous incompressible flows including moving interfaces. The dam break problem is solved by the pseudo-concentration method based on the interface capturing approach. The detailed numerical investigation of the nonlinear solution of the mass conservation equation is presented. The interface sharpening governed by different strategies is examined. The developed mass correction technique is validated on two finite element meshes of different resolution.

A. Каченяускас

СОХРАНЕНИЕ МАССЫ ЖИДКОСТИ В ТЕЧЕНИЯХ С ДВУХСТОРОННЕЙ ПОВЕРХНОСТЬЮ МОДЕЛИРУЕМЫХ ПРИМЕНЯЯ КОНЦЕПЦИЮ НЕВЫРАЖЕННОЙ ПОВЕРХНОСТИ

Р е з ю м е

В статье описывается технология коррекции массы для течения вязких несжимаемых жидкостей с двухсторонней поверхностью. Задача рухнувшей плотины решена при помощи метода псевдоконцентрации, основанного на концепции невыраженной поверхности. Представлен детальный численный анализ решения нелинейного уравнения сохранения массы. Исследовано несколько стратегий управления процедуры реконструкции поверхности. Разработанная технология коррекции массы протестирована на двух сетях конечных элементов различной резолуции.

Received November 05, 2007